Engineering Geology 288 (2021) 106125

Contents lists available at ScienceDirect

Engineering Geology

journal homepage: www.elsevier.com/locate/enggeo

Utilizing the towed Transient ElectroMagnetic method (tTEM) for achieving unprecedented near-surface detail in geological mapping

Peter B.E. Sandersen [a,*], Anders J. Kallesøe [a], Ingelise Møller [a], Anne-Sophie Høyer [a], Flemming Jørgensen [b], Jesper B. Pedersen [c], Anders V. Christiansen [c]

[a] Department of Groundwater and Quaternary Mapping, Geological Survey of Denmark and Greenland (GEUS), C.F. Møllers Allé 8, Building 1110, 8000 Aarhus C, Denmark
[b] Region of Central Denmark, Skottenborg, 8800 Viborg, Denmark
[c] HydroGeophysics Group, Department of Geoscience, Aarhus University, C.F. Møllers Allé 4, 8000 Aarhus C, Denmark

ARTICLE INFO

Keywords:
tTEM
Geological models
Near-surface geophysics
Geological detail
Groundwater vulnerability
Groundwater mapping

ABSTRACT

The subsurface in areas affected by the Pleistocene glaciations often reveal very complex architectures and because of this, the near-surface geology is generally difficult to map and model in high detail. A number of geophysical methods focus on the uppermost part of the subsurface and are capable of mapping details, but no single method has hitherto been able to provide the detail, the data density and the resolution required to map the near-surface Quaternary geology in 3D. Driven by the demands for high detail in the uppermost parts of the subsurface related to for instance surface water and groundwater vulnerability assessments and climate-change related projects, a new high-resolution electromagnetic survey method, tTEM, has been developed. We present examples and discuss the method and its applicability in four study areas where data from tTEM surveys has been combined with geological data and knowledge to map near-surface geological features that could not be resolved in 3D using other geophysical methods focusing on the deeper subsurface or methods with a wider data spacing.

1. Introduction

The subsurface deposits of many areas that were once covered or bordered by Pleistocene ice sheets reveal very complex architectures. During at least the three latest glaciations and the intervening interglacials, multiple episodes of erosion, deposition and deformation have left a marked impact on the upper parts of the subsurface: Glaciotectonic complexes with structural deformation to depths of up to 300–400 m are numerous (e.g. Aber and Ber, 2007; Gehrmann et al., 2019; Pedersen, 2005), and widespread subglacial erosion is evidenced by for instance the occurrence of a large number of buried tunnel valleys eroded to depths of up to 400 m (e.g. Van der Vegt et al., 2012; Jørgensen and Sandersen, 2006). In addition to this, other types of erosion, sedimentation and tectonics have resulted in extensive and complex near-surface sedimentary successions and highly varied terrain morphologies (e.g. Brandes et al., 2018; Houmark-Nielsen, 2007, 2011; Lang et al., 2014; Sandersen and Jørgensen, 2015; Winsemann et al., 2018). Due to this complexity, the upper part of the subsurface geology is generally difficult to map and model in high detail.

Extensive groundwater mapping in Denmark since the mid 90's (Thomsen et al., 2004) created a boost in the development of new geophysical methods that aimed at mapping the uppermost 100–200 m of the subsurface. Developed geophysical methods counted for instance Airborne ElectroMagnetic methods (AEM; e.g. SkyTEM; Danielsen et al., 2003; Sørensen and Auken, 2004), Electrical Resistivity Tomography (ERT; Loke et al., 2013), Induced Polarization (IP; Maurya et al., 2018), Pulled Array Continuous Electrical Sounding (PACES; Christensen and Sørensen, 2001), and ElectroMagnetic Induction (EMI; Christiansen et al., 2016; Doolittle and Brevik, 2014). The development of new methods also spurred new modelling workflows and new ways of combining data (e.g. Sørensen, 1996; Sørensen and Auken, 2004; Jørgensen et al., 2003, 2013; Møller et al., 2009; Høyer et al., 2015a, 2015b; Marker et al., 2015).

Some of the developed geophysical methods focus on the uppermost part of the subsurface and were able to map details, but no method alone could provide the high detail, the high data density and the high resolution that was required to spatially map the complex near-surface Quaternary geology. Therefore, the complexity of the geological

* Corresponding author.
E-mail address: psa@geus.dk (P.B.E. Sandersen).

https://doi.org/10.1016/j.enggeo.2021.106125
Received 17 December 2020; Received in revised form 26 March 2021; Accepted 1 April 2021
Available online 3 April 2021

succession still posed challenges for geo-modellers wanting to create 3D renderings of especially the uppermost 30–50 m (e.g. Høyer et al., 2013b; Jørgensen and Sandersen, 2009).

In vulnerability and climate change related groundwater/surface water interaction projects, there is an increasing demand for highly detailed 3D geological models in order to model groundwater flow and solute transport with the required precision (e.g. Hansen et al., 2016; Refsgaard et al., 2014; Kim et al., 2019; Rasmussen et al., 2020). Likewise, modelling contaminant transport from landfills or industrial facilities require a thorough knowledge of the geological architecture of the upper parts of the subsurface specifically aimed at performing risk evaluations (e.g. Maurya et al., 2017, 2018; Høyer et al., 2019). In Denmark, almost all drinking water is based on groundwater, and the increasing pressure on groundwater resources of high quality therefore defines a new level of detail that 3D geological models are required to meet (Sandersen et al., 2018).

Especially driven by the demands for high detail aimed at assessing surface water and groundwater vulnerability, climate related water challenges, improved modelling of point and surface contamination, a new high-resolution electromagnetic survey method has been developed. The tTEM method (the towed Transient ElectroMagnetic method; Auken et al., 2019; Maurya et al., 2020) has its focus on mapping resistivity variations down to at least 70 m of depth, and it has successfully shown the ability to map the shallow geology at higher levels of resolution than hitherto obtained. In combination with deeper focused geophysics (e.g. SkyTEM; Sørensen and Auken, 2004, Schamper et al., 2014), borehole data and high-resolution terrain models based on LiDAR data (Light Detection and Range; Johnson et al., 2015), new possibilities for gaining an unprecedented level of detail of the near-surface geology are now present.

The high data coverage and the improved resolution of the near-surface geology makes the tTEM method highly suitable for mapping detail to be used in 3D geological models targeted at aquifer mapping, surface water and groundwater vulnerability assessments, climate change adaptation, mapping of aggregates, risk assessments at contaminated sites, construction sites/infrastructure projects etc.

In this paper we present four examples where the tTEM method has added valuable new information of the near-surface geology for use in targeted nitrate regulation and management of agricultural fields, assessments of groundwater vulnerability and groundwater risk assessments related to a contaminated industrial site. The examples focus on geological settings where the tTEM method has been used to map specific near-surface geological features that could not be resolved in 3D using other geophysical methods with a deeper focus or with a less dense data coverage.

2. Selected study areas

The four selected study areas are shown in Fig. 1. The areas are located in glaciated landscapes in western Denmark and represent geological settings in a young glacial landscape from the last glaciation (Weichselian) (Example 3, Ejer Bavnehøj), in old glacial landscapes of the penultimate glaciation (Saalian) (Example 2, Vittarp, and 4, Vildbjerg), and on the lateglacial (Weichselian) outwash plain west of the Main Stationary Line (Example 1, Bolbro). The Main Stationary Line represents the most westerly location of the Scandinavian Ice Sheet during the Late Weichselian (e.g. Houmark-Nielsen, 2007).

The tTEM mapping has been performed as part of projects aimed at mapping and modelling of the fate of nitrogen in groundwater and surface water in agricultural areas (www.MapField.dk; Examples 1 and 3), vulnerability mapping of a deep aquifer, and mapping of near-surface geology for use in risk assessments in relation to a contaminated industrial site (TOPSOIL www.northsearegion.eu/topsoil; Examples 2 and 4).

3. Methods

3.1. The Transient ElectroMagnetic method (TEM)

All developed TEM systems are based on the time-domain electromagnetic method that operates with a large wire loop transmitter and a smaller receiver loop (Danielsen et al., 2003). When a direct current is sent through the transmitter loop, a primary magnetic field is created in the surroundings. When turned off, it induces an eddy current system that diffuse downwards and outwards and decay because of the electric resistance of the ground. This induces a secondary magnetic field that is measured in the receiver loop. This decaying electric field response is related to the conductivity of the subsurface layers and therefore the method provides information of the resistivity distribution of the subsurface (Sørensen and Auken, 2004). Generally, the TEM method provides good resolution of conductive layers, whereas high-resistivity layers are mapped with less precise resistivity estimates (e.g. Jørgensen et al., 2005). The TEM method is sensitive to couplings from the presence of infrastructure such as fences and cables or larger metallic objects (Christiansen et al., 2006), but during standard data processing routines, affected data are removed (Auken et al., 2009).

The TEM methods provide 1D models of the subsurface resistivity variations primarily controlled by the content of clay minerals in the sediment and the ion content of the pore water. Because of overlap between different lithologies in terms of resistivity (Jørgensen et al., 2005; Schamper et al., 2014), heterogeneous sediments, and gradual transitions between lithologies, the conversion of modelled resistivities to specific layer lithology is not straightforward. Also, variations in water saturation and porewater ion content down through the succession can challenge the geological interpretations. Therefore, the modelled resistivity variations must be related to lithological descriptions from boreholes, outcrops, and surface geology maps. If electrical wire-line logs are available from boreholes, resistivity links between the borehole and the TEM data can be performed (e.g. Sandersen et al., 2009; Schamper et al., 2014), thus strengthening local correlations between resistivity and lithology.

For all TEM methods, the survey layout, infrastructure, and area-specific restrictions in accessibility have an impact on data coverage. The system configuration and the resistivity of the subsurface controls the penetration depth as well as the lateral resolution capabilities.

The type of system and the spatial distribution of the collected data thus defines the size of the layers and structures that can be resolved. Generally, the TEM method is only capable of resolving a limited number of layers, and the near-surface layer resolution can – dependent on the chosen configuration – be poor. With depth, there is a decrease in resolution and an increase in footprint, meaning that the modelled resistivities at depth will be the result of averaging over increasingly larger volumes.

In ground-based systems, TEM measurements are typically evenly distributed soundings over an area or soundings along lines, whereas for airborne systems, closely spaced measurements are carried out along flight lines. Each sounding position holds an inverted geophysical layer model with electrical resistivities described in each layer (Danielsen et al., 2003; Auken et al., 2015). Depending on the system configuration, the TEM systems can have varied penetration depths and resolution capabilities. The DOI (Depth of Investigation) is calculated during processing and is available for visualisation along profiles. The DOI illustrates the maximum depth at which the model can be considered reliable (Christiansen and Auken, 2012).

Both ground-based and airborne TEM systems have for more than 25

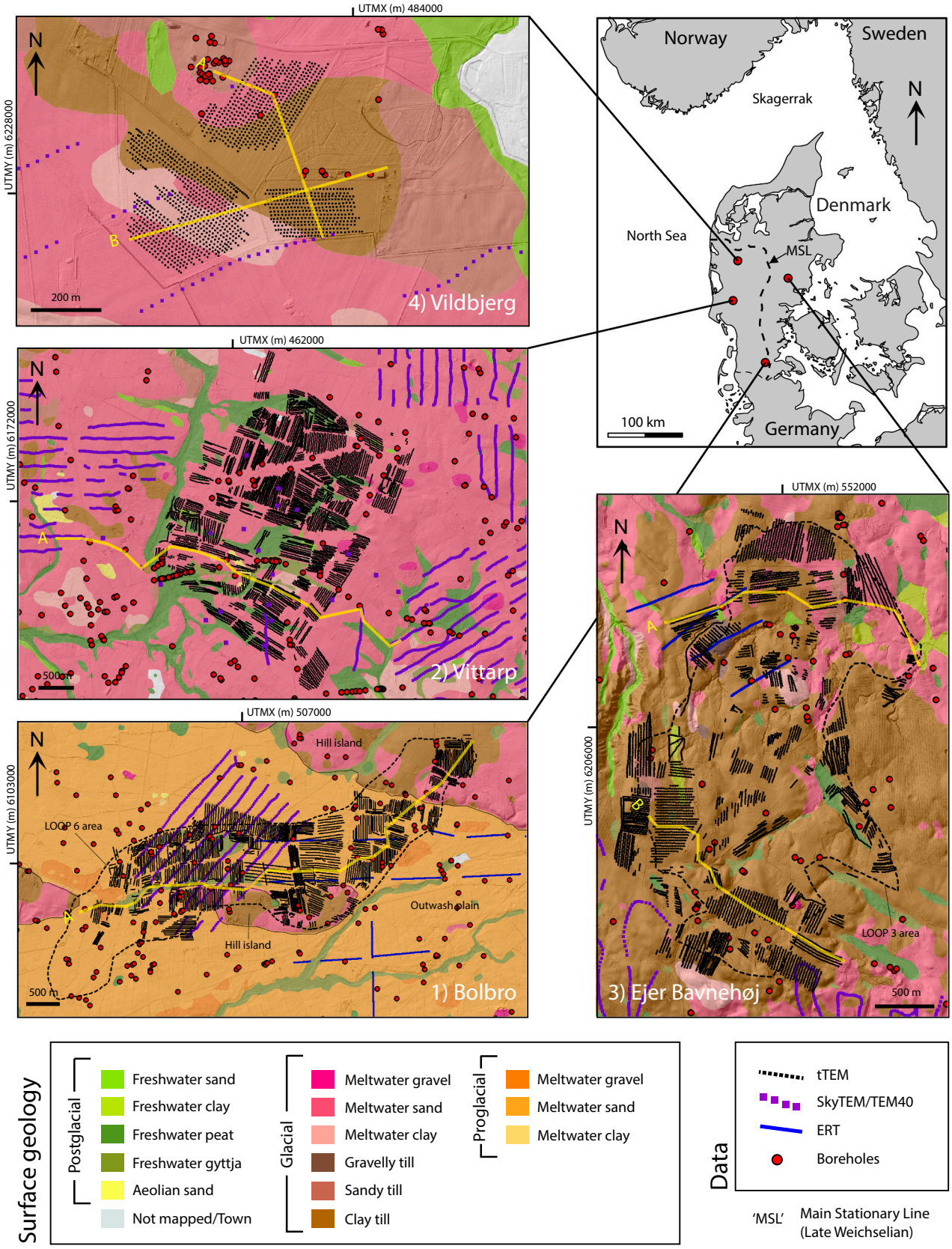

Fig. 1. Location of study areas 1) Bolbro, 2)Vittarp, 3) Ejer Bavnehøj and 4) Vildbjerg. Yellow lines mark locations of the cross-sections shown in Figs. 2 to 5 (Cross-section names in yellow). Surface geology map from Jakobsen and Tougaard (2020). Projection: ETRS89 / UTM zone 32 N. (For interpretation of the references to colour in this figure legend, the reader is referred to the web version of this article.)

years added highly valuable spatial information for use in 3D geological modelling related to the Danish national groundwater mapping programme (Høyer et al., 2011, 2015a, 2015b; Møller et al., 2009; Sandersen and Jørgensen, 2017; Schamper et al., 2014), and has been widely used in mapping projects worldwide (e.g. d'Ozouville et al., 2008; Chandra et al., 2019; Foley et al., 2020; Viezzoli et al., 2009, 2010). For more detail on electromagnetic methods we refer to Christiansen et al. (2006).

3.2. The towed Transient ElectroMagnetic method (tTEM)

The tTEM system is a further development of the TEM method as a down-scaled system that is designed to map from the terrain surface using an ATV (All-Terrain Vehicle) (Auken et al., 2019). The smaller size means a shallower focus depth, and the tTEM system is capable of imaging the uppermost 70 m of the subsurface in high resolution both horizontally and vertically given by its small footprint and dense data collection patterns (Auken et al., 2019).

A typical tTEM survey is done by measuring along lines with a spacing of around 10–25 m and an in-line distance between the soundings of 5–10 m. The versatility of the ATV-mounted equipment is ideal for surveys on almost all types of agricultural fields. Access to fields, however, can in some instances be problematic due to crops, physical obstructions, or lack of entry permissions.

As tTEM is closely related to other TEM systems, inversion, processing, and output is performed using the same workflows (Auken et al., 2019). Basically, the differences lie in the focus depth, the scale at which the TEM systems map and the platform on which the data is collected. The shallow focus of the tTEM makes it the best choice for surveys that target the geology of the near-surface regime, and where highly detailed interpretations are required.

4. Data

4.1. Geophysical data

The tTEM surveys in the study areas have been performed by the Department of Geoscience, Aarhus University. The surveys were done with a standard line spacing in areas dominated by agricultural activities. Due to presence of buried infrastructure, physical obstacles, restrictions in access to fields, and removal of coupled data during the data processing, the data coverage in the four areas varies (Fig. 1). The processed and inverted data were provided as 1D geophysical models in GERDA format (www.geus.dk).

Older geophysical surveys using airborne TEM (SkyTEM), TEM40 or ERT have been performed in or just outside the study areas. Generally, available TEM data has been included in the geological interpretations, but because the ERT data are few, and because the tTEM provides much better resolution and coverage, these data have not been used in the present study.

4.2. Borehole data

The publicly available Danish National Borehole Database 'Jupiter', contains data from more than 280.000 boreholes drilled for multiple purposes spanning a time interval of more than 125 years (Hansen and Pjetursson, 2011). The digital borehole data is hosted by GEUS (www.geus.dk). Symbology and colour coding used in the figures follow GEUS standards.

4.3. Surface geology maps

Digital maps of the surface geology are publicly available in 1:25.000 for 90% of the Danish area (Jakobsen and Tougaard, 2020; www.geus.dk). The maps show interpreted geology and lithology at a depth of approximately 1 m, using standard symbology and colour coding (see Fig. 1).

5. Geological mapping in the selected study areas

5.1. Study area 1, Bolbro: Mapping glaciotectonics and discontinuities within a near-surface succession

5.1.1. Geological setting

The Bolbro area is located on the Late Weichselian Tinglev outwash plain in the southern part of Jutland (Fig. 1). A small part of the study area comprises higher lying remnants of a pre-Weichselian glacial landscape standing out as "hill islands" surrounded by the outwash plain. The outwash plain surface has a gentle slope from east to west. The outwash plain was formed when the Late Weichselian ice sheet was located at the Main Stationary Line (MSL) east of the study area, representing the 'Main ice advance' from northeast (21 kyr BP; Houmark-Nielsen, 2007). The highest parts of the hill islands reach 50 m a.s.l, whereas the outwash plain surrounding the hills is sloping from 35 m in the east to 25 m a.s.l. to the west. Late glacial outwash deposits consisting primarily of sands are dominant, but in the hill islands occurrences of clay till and older meltwater sand can be found. Occurrences of postglacial freshwater deposits can be found locally in topographic lows on the outwash plain. Boreholes reveal Quaternary meltwater sand and gravel, clay tills and postglacial organic rich sediments. At depth, Miocene sequences of marine clays and sands are found.

5.1.2. Geological interpretations

Cross section'Bolbro A' in Fig. 2 gives an overview of the geology of the study area from southwest to northeast. The gentle westerly slope of the outwash plain surrounding the hill islands is clearly seen in the terrain morphology. Hidden below the high-resistive sandy sediments of the outwash plain (a) and the occasional low-resistivity and organic rich Postglacial sediments (b), we find irregularly shaped, low-resistive clay tills and meltwater clays (c). The layers of till and meltwater clay are found throughout the cross-section, except at 1000–1200 m and 4600–4900 m, where the clay apparently has been eroded. Especially in the central part of the cross-section, the layer appears to consist of stacked, northerly/easterly dipping clay slabs creating a highly irregular appearance along the cross-section. The clay forms the core of the hill islands where it can be found at altitudes up to just over 30 m a.s.l., whereas beneath the outwash plain, the top of the clay is found below 20 m a.s.l. The tTEM clearly maps the boundary to the high-resistive sand of the outwash plain above as well as the boundary to the high-resistive meltwater sediments underneath (f). In the hill islands, layers of irregularly shaped, high-resistive layers (d) are found above the clay (c). These layers consist of meltwater sand and gravel, and as seen to the right on the cross-section, they appear to follow the irregular shape of the underlying clay (c).

The calculated standard DOI shows that the tTEM generally maps the succession down to 20 to 50 m b.s.l., and that the deepest model layers show high resistivities (Fig. 2). According to nearby borehole data, the deepest parts of the succession consists of Miocene sands and clays (f) (e.g. Rasmussen et al., 2010), but these layers are not mapped with tTEM because they are located below the DOI.

Friborg (1996) mapped stone-poor, chalk-rich tills of presumed Saalian age beneath the Tinglev outwash plain based solely on borehole data. The surface of these tills mapped by Friborg generally matches the surface of the low resistive clays (c) mapped by tTEM (Fig. 2), but the tTEM data clearly show that the clay is deformed. Glaciotectonically deformed sediments are widespread in southern Denmark (e.g. Andersen et al., 2005; Houmark-Nielsen, 2007; Høyer et al., 2013a; Jørgensen et al., 2015) and since the area has not been overridden by glaciers during the Weichselian the deformations in the study area can be related to the Saalian glaciation. The tTEM shows that the meltwater sediments above the clay in the hill islands are deformed as well. Apart from being deformed, the Saalian clays have also been eroded locally, which means that the clay can be considered as discontinuous and having a highly varied thickness throughout the area.

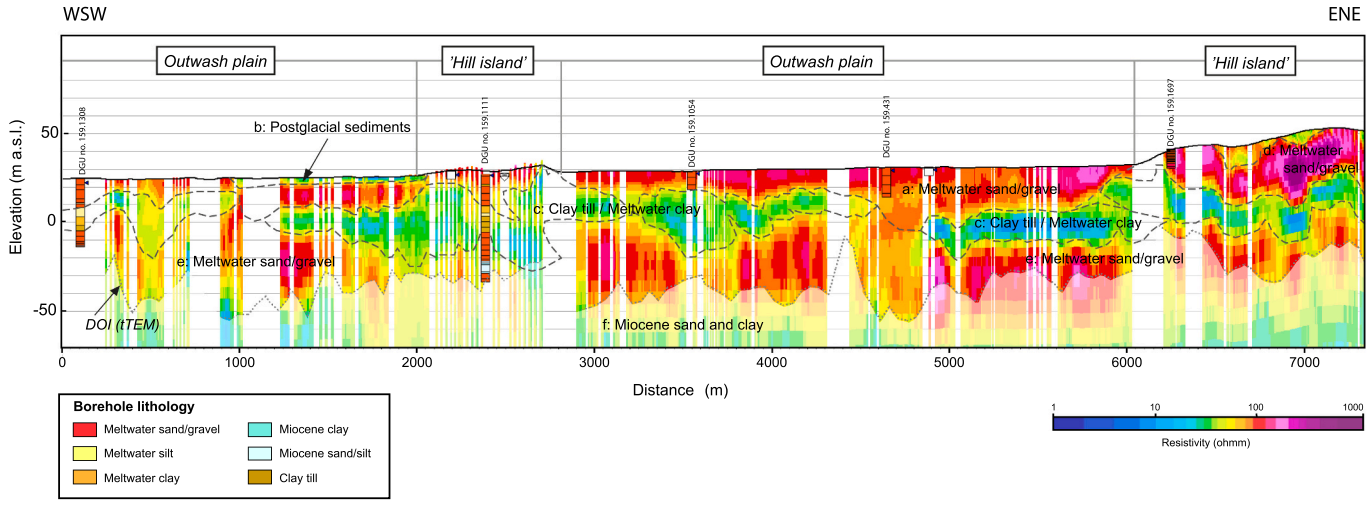

Fig. 2. Cross-section 'Bolbro A', oriented WSW-ENE, 10 X vertical exaggeration. For location, see Fig. 1. TTEM models are shown as coloured vertical 1D soundings. For simplicity, the SkyTEM soundings are not included on the profile. TTEM models below the standard Depth of Investigation (DOI) have been dimmed. Boreholes are shown as coloured vertical rods with database no. above (DGU No.).

Although the tTEM does not map the deep parts of the succession, the highly irregular bottom surface of the Saalian clays points to an equally deformed succession at depth (e and f). This is supported by finds of isolated layers of Miocene sediments within the Quaternary succession, e.g. in borehole DGU No. 159. 1111 (at 2400 m on Fig. 2). The tTEM maps the Lateglacial outwash plain sediments and the spatial boundary to the Saalian sediments in high detail. Locally, the tTEM maps the Postglacial sediments deposited on the outwash plain. Being related to local lows in the outwash plain, the extent of the Postglacial sediments can be further constrained by using LiDAR data.

5.2. *Study area 2, Vittarp: Mapping small erosional valleys at the flanks of a larger valley structure*

5.2.1. *Geological setting*

The Vittarp area is located on a 'hill island' dominated by meltwater sand and gravel with Postglacial freshwater deposits in low-lying parts of the terrain (Fig. 1). The elevation ranges between 5 and 30 m a.s.l. The study area has not been overridden by glaciers during the Weichselian glaciation, and the Late Saalian Warthe ice advance stopped just southwest of the area (Houmark-Nielsen, 2007). SkyTEM data and a

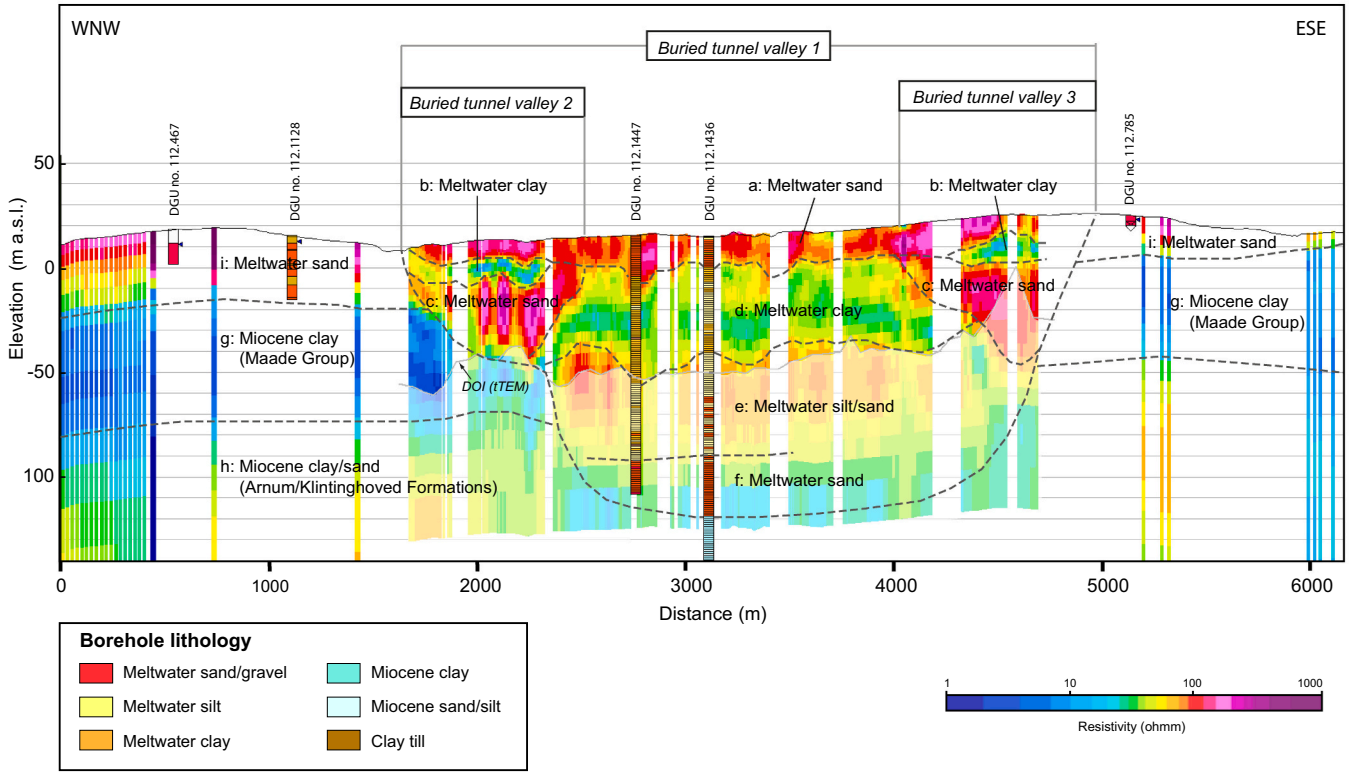

Fig. 3. Cross-section 'Vittarp A', oriented WNW-ESE, 10 X vertical exaggeration. For location, see Fig. 1. TTEM models are shown as coloured vertical 1D soundings between 1600 and 4600 m. The models outside this interval are of TEM40/SkyTEM-type (see Fig. 1). TTEM models below the lower Depth of Investigation (DOI) have been dimmed. Boreholes are shown as coloured vertical rods with database no. above (DGU No.).

limited amount of ground based TEM soundings revealed in combination with seismic data and borehole data a 2–3 km wide and up to 140 m deep buried tunnel valley filled with clayey and sandy Quaternary sediments (Kallesøe et al., 2020). The valley structure is oriented around NE-SW and was interpreted to be at least 15 km long. The valley is eroded down into a Miocene succession of mainly clayey and silty formations (The Maade Group and the Arnum and Klintinghoved Formations; Rasmussen et al., 2010; see Fig. 3).

5.2.2. Geological interpretations

The cross-section 'Vittarp A' (Fig. 3) is located perpendicularly across the buried valley in the southern part of the tTEM mapped area (Fig. 1). Centrally on the cross-section, the more than 2 km wide buried valley structure can be seen eroded down to 120 m b.s.l. The tTEM data maps the resistivity variations down to around 70 m comprising the upper half of the valley infill. The uppermost part of the succession consists of an up to 20 m thick layer of high resistive meltwater sand (a: Meltwater sand) with occasional thin and low resistive patches at the surface. Below the sand, an approximately 40 m thick layer of predominantly low-resistive meltwater clay can be seen in the central part of the valley (d). However, the tTEM reveals that two smaller valley structures appear to be eroded through the meltwater clay (d) and apparently down into the high-resistive meltwater silt and sand below (e). Both valleys are 700–800 m wide and 50–60 m deep, and they are filled with high-resistive meltwater sand (c) and an up to 10–15 m thick layer of meltwater clay (b). The meltwater clay (b) inside the smaller valleys only cover parts of the valleys, and an irregular appearance of the clay indicates erosion and deformation by glaciotectonics. The deepest parts of the broad valley have an infill of meltwater silt (e), and meltwater sand below (f). The tTEM, however, cannot map the deep meltwater sand because it is located below the DOI. The borehole DGU no. 112.1436 at 3100 m on the cross-section shows the meltwater sand (f) and the boundary to the Miocene clay (h) below the valley incision.

In several boreholes around the study area interglacial marine sediments from the Holsteinian interglacial have been described. In a borehole 1½ km south of Profile Vittarp A (DGU no. 112.625) and thus within the buried valley structure, marine interglacial clay has been described from 16 to 23 m b.s.l. This could suggest an Elsterian age of the large, buried valley and infilling during the Elsterian glaciation and the following Holsteinian interglacial. The sandy and silty infill of the deep parts of the large, buried valley was therefore probably deposited during the Elsterian (layers e and f), and the meltwater clay (d) may possibly be correlated with Late Elsterian/Holsteinian clays. This would, in turn, point to a Saalian age for the two smaller valleys, formed along the boundaries of the older and broader buried valley. The infill of the small valleys, the sand above the valleys, and the proposed glaciotectonic deformations are therefore most likely related to the Saalian glaciation.

5.3. Study area 3, Ejer Bavnehøj: Mapping buried valley infill sediments

5.3.1. Geological setting

The Ejer Bavnehøj study area is located in a hilly glaciated landscape reaching elevations of 170 m a.s.l. to the south and sloping down to around 40 m a.s.l. to the northeast (Fig. 1). The hilly terrain is dominated by orientations perpendicular to the slope (WNW-ESE to N-S), and in a few places, erosional valleys are seen parallel to the slope (WSW-ENE to SW-NE). According to the surface geology map, clay tills dominate but occurrences of meltwater sand can be found in the lowest parts of the terrain to the north. Postglacial freshwater deposits can be found locally. The two latest ice-advances that reached the area was the 'Main ice advance' from northeast and later the 'East Jutland advance' from southeast (Larsen et al., 1979). The ice-advance from northeast had a temporary ice margin approximately at the culmination of the hills, whereas the ice from southeast is interpreted to have stopped just east of the study area.

Boreholes show that the deep parts of the subsurface consist of Eocene marine clay. Above this clay, scattered and thin occurrences of presumably Oligocene mica clay are found. The Quaternary succession above consists of predominantly clayey tills, meltwater sand, meltwater gravel, and minor occurrences of meltwater clay. Isolated slabs of pre-Quaternary sediments occur occasionally within the Quaternary succession suggesting glaciotectonic deformation. The thickness of the Quaternary succession ranges from a few meters to more than 100 m.

5.3.2. Geological interpretations

Despite a patchy tTEM coverage caused by mapping restrictions in certain areas, the tTEM provides a good resolution of individual layers and the surface of the good conductor. Unfortunately, the information from boreholes are limited because many of the boreholes are shallow, but in combination with the tTEM, the general perception of the succession is good.

The cross-section 'Ejer Bavnehøj A' in Fig. 4 (see location on Fig. 1), crosses a narrow and a wide buried valley to the north in the study area. The narrow valley to the left has an infill dominated by tills, whereas the broad valley to the right has a mixed and irregular infill of sand and clay layers. Please note that as the orientation of the valley to the right is ESE-WNW and because the cross-section cuts the valley at an oblique angle, the valley appears very wide. The tTEM data shows a more complex architecture of the valley infill which contrasts with the more or less undeformed infill of the valleys to the south (see cross-section B).

The cross-section 'Ejer Bavnehøj B' (Fig. 4; see location on Fig. 1) sums up the geology of the highest parts of the terrain. The Eocene clay stands out as the deep good conductor in the tTEM data. Several valleys have been eroded into the Eocene clay, giving it an undulating surface. The Quaternary succession above the Eocene clay consists of layers of alternating low and high resistivities and based on nearby boreholes and the surface geology map, this corresponds to tills, meltwater sands/clays and occasional occurrences of postglacial freshwater deposits. On the cross-section, the infill of the valleys appears to be of the same type and build and apparently only slightly deformed.

Generally, the effects of glaciotectonic deformation from a northeasterly direction by the 'Main ice advance' has left its mark on the terrain as pronounced orientations of hill crests and slopes.

5.4. Study area 4, Vildbjerg: Mapping the continuity of near-surface Miocene clay sediments

5.4.1. Geological setting

The Vildbjerg study area is located in a glacial landscape west of the MSL that has been exposed since the Saalian glaciation (e.g. Houmark-Nielsen, 2011) (Fig. 1). The terrain is smooth with elevations between 40 and 50 m a.s.l., and the surface geology shows coarse meltwater deposits and patches of clay till and meltwater clay, and with freshwater deposits in topographic lows. Boreholes in the area indicate that the Quaternary sediments are only a few meters thick and consist of clay till and meltwater sand (e.g. borehole DGU no. 84.1954; cross-section A, Fig. 5). Below, boreholes show a pre-Quaternary succession of alternating layers of Miocene mica clay and quarts-rich sand (e.g. DGU no. 84.1953; cf. Rasmussen et al., 2010, Cross-section B, Fig. 5). Deeply eroded buried tunnel valleys found close to the study area (Sandersen and Jørgensen, 2017; www.buriedvalleys.dk) and the limited thickness of glacial sediments above the Miocene layers indicate intense erosion during the Quaternary.

5.4.2. Geological interpretations

The two profiles show presence of a continuous clay layer in the uppermost part of the pre-Quaternary succession between 15 and 40 m a.s.l. as interpreted from tTEM models and borehole data. The clay layer is present everywhere in all the three surveyed sub-areas (see Fig. 1) and is between 5 and 25 m thick. The exceptionally low resistivity indicates that the clay content is high and that it can be considered almost

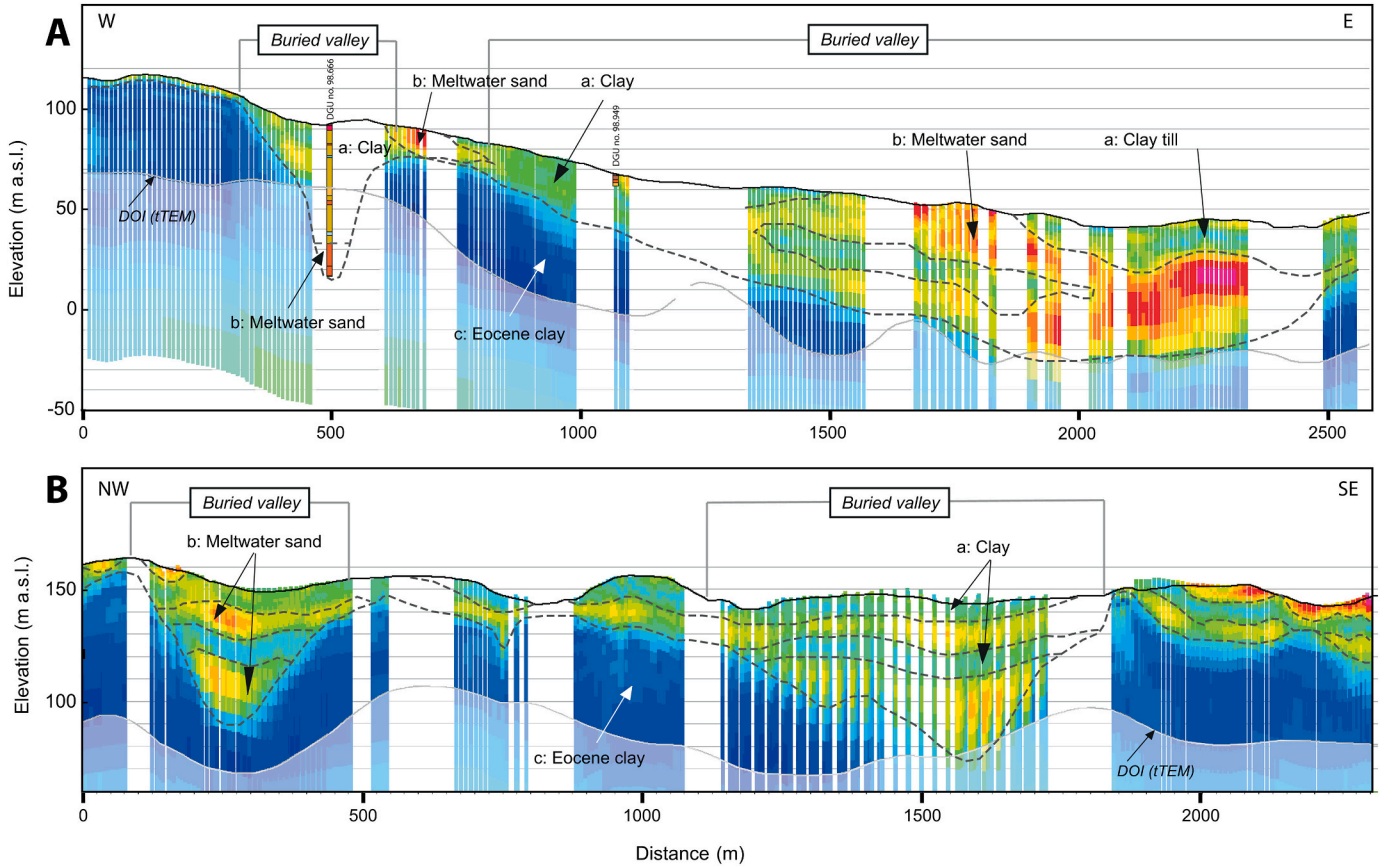

Fig. 4. Cross-sections Ejer Bavnehøj A and B, oriented W-E and NW-SE, respectively. 4 X vertical exaggeration. For location, see Fig. 1. TTEM models are shown as coloured vertical 1D soundings. For legend, see Fig. 2. TTEM models below the Depth of Investigation (DOI) have been dimmed. Boreholes are shown as coloured vertical rods with database no. above (DGU No.).

impermeable. Lithological information from boreholes confirm the presence of the clay and descriptions state that the clay is blackish brown, sticky, non-calcareous and contains mica (DGU No. 84.1953). The clay appears to be practically undeformed and continuous in the mapped area. The deeper Miocene layers are dominated by sand, but with occurrences of clay that appears less continuous in data (see profiles on Fig. 5). The lithology of the clay in the deeper Miocene layers matches the clay above (DGU No. 84.1953), but the thickness is below 15 m. A layer of less than 15 m at this depth is at the limit of what can be resolved with the tTEM system, and this is thought to be the reason for its inconsistent appearance. It is likely, that the layer cannot be resolved properly in areas where the thickness is less than the resolution allows and that it exists all over the area, without being visible in data everywhere. The slightly higher resistivity of the layer (compared to the upper clay layer), can also be ascribed to limitations in resolution at depth.

5.5. Summary of the geological interpretations

The tTEM mapping at the selected study areas show a variety of sandy and clayey geological settings where glaciotectonic deformation and erosional and depositional events during the Quaternary have had a significant impact. The delineation of the complexity of the pre-Weichselian succession in the Bolbro study area (1) is an important find revealed by tTEM. As mentioned earlier, glaciotectonic deformations have been found in several places in southern Jutland, but with the Bolbro area added to this picture, the area in which pre-Weichselian glaciotectonism can be expected is considerably enlarged. In relation to the objective of the mapping, the tTEM has also provided a more detailed mapping of surficial, organic rich postglacial sediments, which is important for studies of the transport of nitrate from agricultural activities in groundwater and surface water. The mapping at Bolbro showed the best resolution of the uppermost 50 m of the subsurface, whereas the deeper parts were dominated by large variations in resistivity and a general lack of borehole data. However, the gained information of the deformed near-surface sediments lead to the conclusion that the heterogenous appearance of the deep parts was the result of equally intense glaciotectonic deformation at depth. This was supported by borehole data.

At the Vittarp study area (2), the tTEM mapping provided a detailed delineation of two generations of buried valleys and enabled an interpretation of a series of erosional and depositional events. The youngest generation of buried valleys was found to be narrow and eroded down into the sediments of the wider, deeper, and older buried valley. The young generation was mainly sand-filled and situated close to the terrain. The detailed spatial picture of the near-surface sedimentary succession has therefore been important for assessments of the vulnerability of the deep buried valley aquifer at the site. The example shows the importance of mapping the near-surface architecture and lithological variations. The deep parts of the deep valley holding the aquifer, however, could not be delineated by the tTEM survey because of the considerable depth. Here, the information was provided by deep boreholes and other more deeply focused TEM.

Despite the patchy coverage with tTEM and the limited number of boreholes at the Ejer Bavnehøj study area (3), the data provided a good resolution of individual layers within the buried valleys and a good contrast to the deep, good electrical conductor represented by the Palaeogene clay. The data improved the understanding of the infill of the valleys and has revealed different degrees of complexity. Although the narrow and shallow valleys eroded into the low-resistive Palaeogene clay were not known beforehand, the observations fit well into the

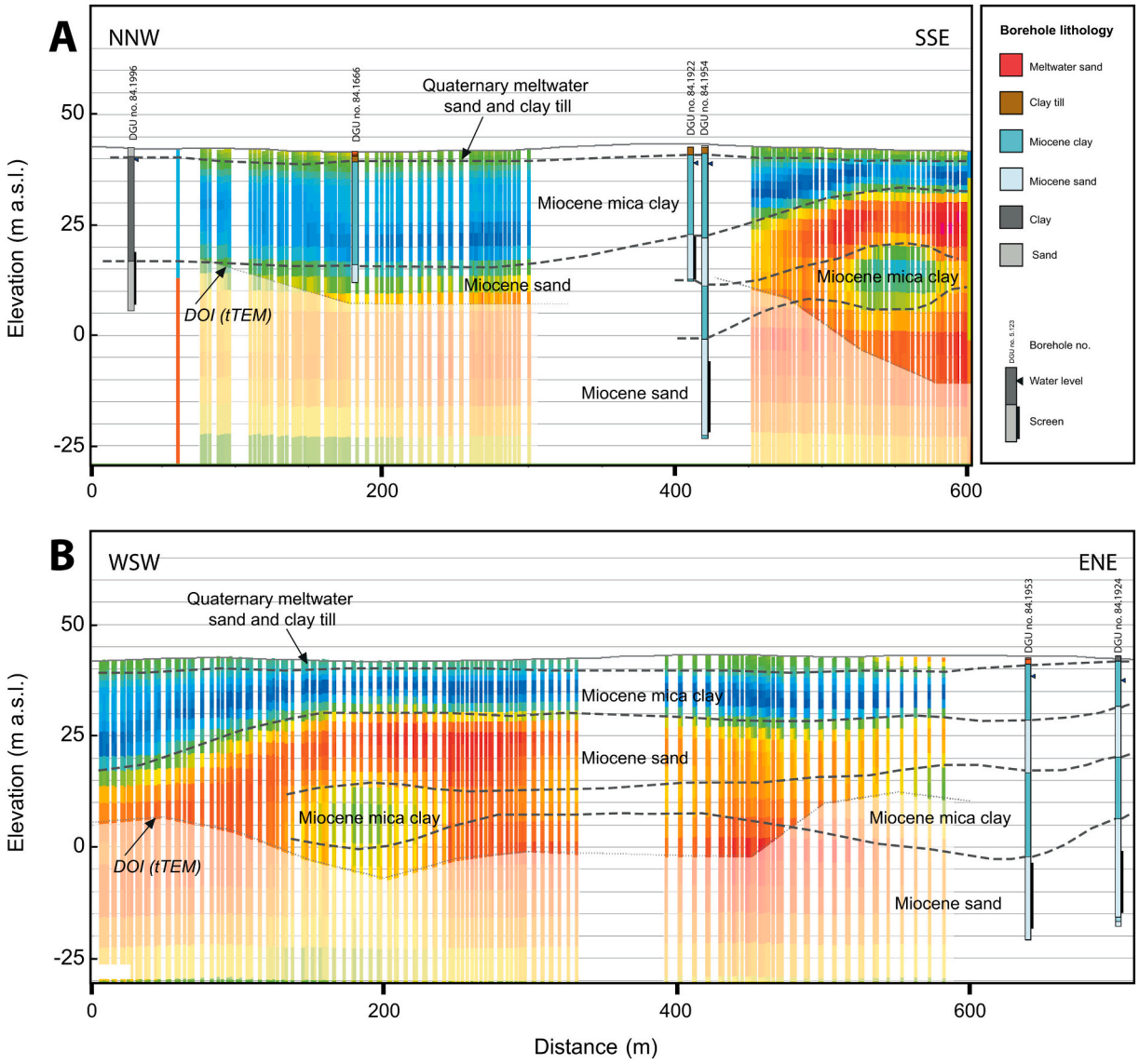

Fig. 5. Two profiles across the Vildbjerg site. 3 X vertical exaggeration. For location, see Fig. 1. TTEM models are shown as coloured vertical 1D soundings (for resistivity legend, see Fig. 2). TTEM models below the Depth of Investigation (DOI) have been dimmed. Boreholes are shown as coloured vertical rods with database no. above (DGU No.).

current knowledge of the latest geological events in the area, thus providing robust geological correlations between the geological and geophysical data.

At the Vildbjerg study area (4), the tTEM mapping revealed the presence of an almost undisturbed and widespread clay layer very close to the terrain surface. Boreholes confirm the presence of the clay layer describing it as Miocene clay. The undisturbed nature of the clay was important for the subsequent risk assessments related to contaminants at an industrial site located on top of the mapped succession (Maurya et al., 2020). In contrast to the other three study areas, the complexity of the geology at this site was low, but nonetheless, a confirmation of exactly this was important new knowledge.

6. Discussion

6.1. Comparisons between tTEM and other geophysical methods

In contrast to deep focused TEM systems the tTEM system focuses on the uppermost tens of metres of the subsurface with the DOI correspondingly shallow. Other systems may be able to resolve near-surface geological features in 2D or 3D depending on their size (e.g. Loke et al., 2013; Revil et al., 2012; Christensen and Sørensen, 2001; Christiansen et al., 2016; Doolittle and Brevik, 2014), but when it comes to mapping features in 3D, the tTEM is capable of providing high layer resolution, high data coverage as well as a considerable penetration depth (see Auken et al., 2019). Compared to the tTEM penetration depth of at least 70 m, the EMI and PACES reach down to depths of a few meters and down to around 25 m, respectively. Although some airborne TEM systems such as SkyTEM, has undergone developments aimed at adding more resolution of the near-surface layers, the flight line spacing and the larger footprint compared to small land-based methods impede near-surface resolution (e.g. Christensen, 2014; Schamper et al., 2014).

When comparing methods, however, it should be remembered that the different geophysical methods are targeting areas at very different scales – from deep, regional surveys using airborne TEM to local near-surface mapping using EMI, PACES or tTEM. Choosing between or choosing both a shallow and a deeper focused survey, therefore strongly depends on the purpose of the mapping. The tTEM system provides a tool that supplements existing geophysical mapping methods targeted at the deeper parts of the subsurface. In Denmark, the tTEM data can, as e.

g., shown in the Vittarp example, be directly compiled with other TEM data due to a calibration of all Danish TEM instruments at a national test site before each mapping campaign (Foged et al., 2013). This calibration procedure and standards for data collection and processing lead to 'absolute' resistivities for all TEM data (e.g. Møller et al., 2009). It is not in the same way, possible to obtain comparable resistivities, when collecting data using electromagnetic frequency domain systems like EMI systems.

The high data coverage and the improved layer resolution in the near-surface parts makes the tTEM method stand out as a mapping method that provides adequate detail for 3D geological interpretations targeted at for instance near-surface mapping for targeted regulation of agriculture, aquifer mapping, groundwater vulnerability assessments, climate change adaptation, mapping of aggregates, and risk assessments at contaminated sites.

6.2. Challenges and opportunities

The tTEM method shares the challenges of accessibility with other land based geophysical methods (e.g. Maurya et al., 2020). Where airborne surveys can be performed more or less without interfering with activities at the surface and without negative impact from land use, the land-based methods rely on factors such as general physical accessibility, crop seasons, waterlogging, and above all, granted access from farmers. To get the farmers accept, it is important that the data collection can be performed without damaging crops, fields, and access roads. As the tTEM equipment is towed on a sledge behind an ATV along the driving tracks in the fields, damage to the crops is usually minimal. In some areas, such as Ejer Bavnehøj (3), restricted access resulted in a patchy data coverage (see Fig. 1), but despite that, the survey resulted in an improved geological understanding of the area.

Limitations of the TEM method in general, such as the averaging of electrical resistivities over increasingly larger volumes with depth and the difficulties relating a modelled layer resistivity to a specific lithology is also present for tTEM. However, with the improved resolution of the near-surface geology with tTEM, it is possible to perform more precise correlations with borehole lithology, surface geology and topography and thereby gain more new information on geological architecture.

Mapping more detail means the likely emergence of new geological structures that hitherto have remained unrecognized. Although this is part of the actual purpose of the mapping, the higher detail and complexity in the subsurface architecture can lead to new questions and challenges such as: How do the new and smaller structures relate to the larger and previously known structures in terms of formation, how do they fit into the event chronology, and how can we ensure optimal use of the detailed subsurface information in the 3D geological model? The answers will inevitably be as varied as the mapped areas and the purposes of the mapping, but in each case the fieldwork and choice of mapping methods should be balanced carefully with the level of detail needed in the 3D models. This will help specifying the mapping strategy and selecting the best 3D mapping approach for the specific study area.

An important thing in relation to 3D geological mapping is to choose the best combination of methods in order to gain the highest possible resolution in the shallow as well as the deep parts of the subsurface. The differently focused geophysical methods will create different data sets that can supplement each other. Depending on the data quality and the character of the subsurface there will be an overlap between the target intervals of the individual mapping methods. The success of the mapping effort depends on how well the target geological structures can be resolved, and specifically in relation to the electrical and electromagnetic methods, this depends largely on the chosen method, the target size and the resistivity contrasts of the geological setting.

As the examples from the study areas show, the tTEM surveys resulted in highly detailed renderings of complex subsurface resistivity variations. However, the full advantage is not gained until the resistivity variations have been combined with lithology from boreholes, surface geology maps, and the topography. This combination of data allows for a better lithological interpretation of resistivities and provides the basis for improved geological correlations inside as well as outside the surveyed area. The geological interpretations also enable the creation of a local geological event chronology that fits into the regional geological knowledge. This is crucial when establishing high detail 3D geological models of near-surface layers aimed at solving problems related to for instance groundwater and surface water vulnerability, where local geological variations can be critical. A thorough understanding of the geology will also enable the modeller to make qualified interpretations in areas without data.

The introduction of the tTEM method and the new possibilities of mapping detailed 3D geology will most likely lead to continued development of geophysical mapping methods and inspire to development of new approaches and workflows for constructing 3D geological models.

7. Conclusions

With the development of the tTEM method capable of delivering an unprecedented high degree of detail of the near-surface succession, the possibilities of mapping the uppermost 50 to 70 m in 3D are now better than ever. The tTEM method fills a gap in the geophysical toolbox, and – as shown in the examples - it fits nicely into the geologist's set of tools as well when facing shallow subsurface mapping challenges related to different types of mapping projects.

The presented examples illustrate the capabilities of the tTEM method to map complex near-surface geology, and especially Quaternary geological settings dominated by deformation and multiple episodes of erosion and deposition. The tTEM data were co-interpreted with surface geology maps, highly detailed digital elevation models, borehole data and in some cases the deeper focused TEM/SkyTEM data, thereby facilitating an understanding of the series of geological events responsible for the formation of the near-surface sedimentary succession. The tTEM method will not only improve the knowledge of the near-surface geology and the events that formed it, but it will also contribute to a better link with the deeper parts of the subsurface.

With the tTEM method, the ability of making detailed 3D geological models of the uppermost 50 to 70 m has been greatly improved. There is an increasing demand for highly detailed near-surface geological models for solving challenges related to for instance aggregates, groundwater resources, and soil and groundwater contamination. Especially in cases where focus is on assessments of groundwater and surface water vulnerability to unwanted chemical compounds from the surface, it is for example very important to be able to locally confirm whether protecting clay layers are continuous or not.

Declaration of Competing Interest

The authors declare that they have no known competing financial interests or personal relationships that could have appeared to influence the work reported in this paper.

Acknowledgements

We thank TOPSOIL, an Interreg project supported by the North Sea Programme of the European Regional Development Fund of the European Union, and the Mapfield Project (Field scale mapping for targeted N-regulation and management), funded by the Danish Innovation Fund (Award number 8855-00025), for supporting this publication economically and for allowing us to publish project results.

We thank editor Janusz Wasowski and two anonymous reviewers for very constructive comments and suggestions that helped improving the manuscript. We also thank Birgitte Hansen, GEUS, for helpful comments and Kenneth Ejsbøl from Din Forsyning for fruitful discussions and for allowing us to use their data.

References

Aber, J.S., Ber, A., 2007. Glaciotectonism. Developments in Quaternary Sciences, 6. Elsevier, p. 246. ISBN-13: 978-0-444-52943-5.

Andersen, L.T., Hansen, D.L., Huuse, M., 2005. Numerical modelling of thrust structures in unconsolidated sediments: implications for glaciotectonic deformation. J. Struct. Geol. 27, 587–596. https://doi.org/10.1016/j.jsg.2005.01.005.

Auken, E., Christiansen, A.V., Westergaard, J.A., Kirkegaard, C., Foged, N., Viezzoli, A., 2009. An integrated processing scheme for high-resolution airborne electromagnetic surveys, the SkyTEM system. Explor. Geophys. 40, 184–192. https://doi.org/10.1071/EG08128.

Auken, E., Christiansen, A.V., Fiandaca, G., Schamper, C., Behroozmand, A.A., Binley, A., Nielsen, E., Effersø, F., Christensen, N.B., Sørensen, K.I., Foged, N., Vignoli, G., 2015. An overview of a highly versatile forward and stable inverse algorithm for airborne, ground-based and borehole electromagnetic and electric data. Explor. Geophys. 46, 223–235. https://doi.org/10.1071/EG13097.

Auken, E., Foged, N., Larsen, J.J., Lassen, K.V.T., Maurya, P.K., Dath, S.M., Eiskjær, T.T., 2019. tTEM — A towed transient electromagnetic system for detailed 3D imaging of the top 70 m of the subsurface. Geophysics 84 (1), E13–E22. https://doi.org/10.1190/geo2018-0355.1.

Brandes, C., Steffen, H., Sandersen, P.B.E., Wu, P., Winsemann, J., 2018. Glacially induced faulting along the NW segment of the Sorgenfrei-Tornquist Zone, northern Denmark: Implications for neotectonics and Lateglacial fault-bound basin formation. Quat. Sci. Rev. 189, 149–168. https://doi.org/10.1016/j.quascirev.2018.03.036.

Chandra, S., Auken, E., Maurya, P.K., Ahmed, S., Verma, S.K., 2019. Large Scale Mapping of Fractures and Groundwater Pathways in Crystalline Hardrock by AEM. Sci. Rep. 9, 398. https://doi.org/10.1038/s41598-018-36153-1.

Christensen, N.B., 2014. Sensitivity functions of transient electromagnetic methods. Geophysics 79 (4). https://doi.org/10.1190/geo2013-0364.1.

Christensen, N.B., Sørensen, K.I., 2001. Pulled array continuous electrical sounding with an additional inductive source: An experimental design study. Geophys. Prospect. 49, 241–254. https://doi.org/10.1046/j.1365-2478.2001.00257.x.

Christiansen, A.V., Auken, E., 2012. A global measure for depth of investigation. Geophysics (4), 77. https://doi.org/10.1190/geo2011-0393.1.

Christiansen, A.V., Auken, E., Sørensen, K.I., 2006. The transient electromagnetic method. In: Kirsch, R. (Ed.), Groundwater Geophysics. A Tool for Hydrogeology. Springer Verlag, Berlin, pp. 179–224. ISBN 10: 3–540–29383-3.

Christiansen, A.V., Pedersen, J.B., Auken, E., Søe, N.E., Holst, M.K., Kristiansen, S.M., 2016. Improved geoarchaeological mapping with electromagnetic induction instruments from dedicated processing and inversion. Remote Sens. 8, 1022. https://doi.org/10.3390/rs8121022.

Danielsen, J.E., Auken, E., Jørgensen, F., Søndergaard, V.H., Sørensen, K.I., 2003. The application of the transient electromagnetic method in hydrogeophysical surveys. J. Appl. Geophys. 53, 181–198. https://doi.org/10.1016/j.jappgeo.2003.08.004.

Doolittle, J.A., Brevik, E.C., 2014. The use of electromagnetic induction techniques in soils studies. Geoderma 223–225, 33–45. https://doi.org/10.1016/j.geoderma.2014.01.027.

d'Ozouville, N., Auken, E., Sørensen, K.I., Violette, S., Marsily, G.D., Deffontaines, B., Merlen, G., 2008. Extensive perched aquifer and structural implications revealed by 3D resistivity mapping in a Galapagos volcano. Earth Planet. Sci. Lett. 269, 518–522. https://doi.org/10.1016/j.epsl.2008.03.011.

Foged, N., Auken, E., Christiansen, A., Sørensen, K., 2013. Test-site calibration and validation of airborne and ground-based TEM systems. Geophysics 78, E95–E106. https://doi.org/10.1190/GEO2012-0244.1.

Foley, N., Tulaczyk, S., Auken, S., Grombacher, D., Mikucki, J., Foged, N., Myers, K., Dugan, H., Doran, P.T., Virginia, R.A., 2020. Mapping geothermal heat flux using permafrost thickness constrained by airborne electromagnetic surveys on the western coast of Ross Island. Antarctica. 51 (1), 84–93. https://doi.org/10.1080/08123985.2019.1651618.

Friborg, R., 1996. The landscape below the Tinglev outwash plain: a reconstruction. Bull. Geol. Soc. Den. 43, 34–40.

Gehrmann, A., Meschede, M., Hüneke, H., Pedersen, S.A.S., 2019. Sea cliff at Kieler Ufer (Pleistocene stripes 11–16) – Large-scale Architecture and Kinematics of the Jasmund Glacitectonic Complex, 2. DEUQUA Spec. Pub., pp. 19–27. https://doi.org/10.5194/deuquasp-2-19-2019

Hansen, B., Sonnenborg, T.O., Møller, I., Bernth, J.D., Høyer, A.-S., Rasmussen, P., Sandersen, P.B.E., Jørgensen, F., 2016. Nitrate vulnerability assessment of aquifers. Environ. Earth Sci. 75, 999. https://doi.org/10.1007/s12665-016-5767-2.

Hansen, M., Pjetursson, B., 2011. Free, online Danish shallow geological data. Geol. Surv. Denm. Greenl. Bull. 23, 53–56. https://doi.org/10.34194/geusb.v23.4842.

Houmark-Nielsen, M., 2007. Extent and age of Middle and late Pleistocene glaciations and periglacial episodes in southern Jylland, Denmark. Bull. Geol. Soc. Denmark 55, 9–35.

Houmark-Nielsen, M., 2011. Pleistocene Glaciations in Denmark: A Closer Look at Chronology, Ice Dynamics and Landforms. Developments in Quaternary Science. vol. 15. Doi: https://doi.org/10.1016/B978-0-444-53447-7.00005-2. ISSN: 1571-0866, Elsevier B.V.

Høyer, A.-S., Lykke-Andersen, H., Jørgensen, F., Auken, E., 2011. Combined interpretation of SkyTEM and high-resolution seismic data. Phys. Chem. Earth 36, 1386–1397. https://doi.org/10.1016/j.pce.2011.01.001.

Høyer, A.-S., Jørgensen, F., Piotrowski, J.A., Jakobsen, P.R., 2013a. Deeply rooted glaciotectonism in western Denmark: geological composition, structural characteristics and the origin of Varde hill-island. J. Quat. Sci. 28, 683–696. https://doi.org/10.1002/jqs.2667.

Høyer, A.-S., Møller, I., Jørgensen, F., 2013b. Challenges in geophysical mapping of glaciotectonic structures. Geophysics 78 (5), B287–B303. https://doi.org/10.1190/geo2012-0473.1.

Høyer, A.-S., Jørgensen, F., Foged, N., He, X., Christiansen, A.V., 2015a. Three-dimensional geological modelling of AEM resistivity data - a comparison of three methods. J. Appl. Geophys. 115, 65–78. https://doi.org/10.1016/j.jappgeo.2015.02.005.

Høyer, A.-S., Jørgensen, F., Sandersen, P.B.E., Viezzoli, A., Møller, I., 2015b. 3D geological modelling of a complex buried-valley network delineated from borehole and AEM data. J. Appl. Geophys. 122, 94–102. https://doi.org/10.1016/j.jappgeo.2015.09.004.

Høyer, A.-S., Klint, K.E.S., Fiandaca, G., Maurya, P.K., Christiansen, A.V., Balbarini, N., Bjerg, P.L., Hansen, T.B., Møller, I., 2019. Development of a high-resolution 3D geological model for landfill leachate risk assessment. Eng. Geol. 249, 45–59. https://doi.org/10.1016/j.enggeo.2018.12.015.

Jakobsen, P.R., Tougaard, L., 2020. Danmarks digitale jordartskort (Surface geology map), 1:25000, Version 5.0. Geological Survey of Denmark, p. 29. Report 2020/18.

Johnson, M.D., Fredin, O., Ojala, A.E.K., Peterson, G., 2015. Unraveling Scandinavian geomorphology: the LiDAR revolution. GFF 137, 245–251. https://doi.org/10.1080/-11035897.2015.1111410.

Jørgensen, F., Sandersen, P., 2006. Buried and open tunnel valleys in Denmark – erosion beneath multiple ice sheets. Quat. Sci. Rev. 25, 1339–1363. https://doi.org/10.1016/j.quascirev.2005.11.006.

Jørgensen, F., Sandersen, P.B.E., 2009. Buried valley mapping in Denmark: evaluating mapping method constraints and the importance of data density. Z. Dtsch. Ges. Geowiss. 160, 211–223. https://doi.org/10.1127/1860-1804/2009/0160-0211.

Jørgensen, F., Lykke-Andersen, H., Sandersen, P.B.E., Auken, E., Nørmark, E., 2003. Geophysical investigations of buried Quaternary valleys in Denmark: an integrated application of transient electromagnetic Geophysical soundings, reflection seismic surveys and exploratory drillings. J. Appl. Geophys. 53 (4), 215–229. https://doi.org/10.1016/j.jappgeo.2003.08.017.

Jørgensen, F., Sandersen, P.B.E., Auken, E., Lykke-Andersen, H., Sørensen, K., 2005. Contributions to the geological mapping of Mors, Denmark – a study based on a large-scale TEM survey. Bull. Geol. Soc. Denm. 52, 53–75. https://doi.org/10.37570/bgsd-2005-52-06.

Jørgensen, F., Møller, R.R., Nebel, L., Jensen, N., Christiansen, A.V., Sandersen, P., 2013. A method for cognitive 3D geological voxel modelling of AEM data. Bull. Eng. Geol. Environ. 72, 421–432. https://doi.org/10.1007/s10064-013-0487-2.

Jørgensen, F., Høyer, A.-S., Sandersen, P.B.E., He, X., Foged, N., 2015. Combining 3D geological modelling techniques to address variations in geology, data type and density – an example from Southern Denmark. Comput. Geosci. 81 (2015), 53–63. https://doi.org/10.1016/j.cageo.2015.04.010.

Kallesøe, A.J., Rasmussen, P., Sandersen, P., Sonnenborg, T.O., 2020. Varde - Vittarp – 3D Geologisk Model og Hydrologisk Model. Et Pilotområde i INTERREG Projekt TOPSOIL. Geological Survey of Denmark and Greenland, p. 88. Report 2020/14.

Kim, H., Høyer, A.-S., Jakobsen, R., Thorling, L., Aamand, J., Maurya, P.K., Christiansen, A.V., Hansen, B., 2019. 3D characterization of the subsurface redox architecture in complex geological settings. Sci. Total Environ. 693 (2019), 133583. https://doi.org/10.1016/j.scitotenv.2019.133583.

Lang, J., Hampel, A., Brandes, C., Winsemann, J., 2014. Response of salt structures to icesheet loading: implications for ice-marginal and subglacial processes. Quat. Sci. Rev. 101, 217–233. https://doi.org/10.1016/j.quascirev.2014.07.022.

Larsen, G., Kronborg, C., Bender, H., 1979. Det midtjyske Søhøjland. Geol. Århus Amtskom. Amtsfredningskontoret. Oktober 1979. ISBN 87-980867-0-7.

Loke, M.H., Chambers, J.E., Rucker, D.F., Kuras, O., Wilkinson, P.B., 2013. Recent developments in the direct-current geoelectrical imaging method. J. Appl. Geophys. 95, 135–156. https://doi.org/10.1016/j.jappgeo.2013.02.017.

Marker, P.A., Foged, N., He, X., Christiansen, A.V., Refsgaard, J.C., Auken, E., Bauer-Gottwein, P., 2015. An automated method to build groundwater model hydrostratigraphy from airborne electromagnetic data and lithological borehole logs. Hydrol. Earth Syst. Sci. Discuss. 12, 1555–1598. https://doi.org/10.5194/hessd-12-1555-2015.

Maurya, P.K., Rønde, V.K., Fiandaca, G., Balbarini, N., Auken, E., Bjerg, P.L., Christiansen, A.V., 2017. Detailed landfill leachate plume mapping using 2D and 3D electrical resistivity tomography-with correlation to ionic strength measured in screens. J. Appl. Geophys. 138, 1–8. https://doi.org/10.1016/j.jappgeo.2017.01.019.

Maurya, P.K., Balbarini, N., Møller, I., Rønde, V., Christiansen, A.V., Bjerg, P.L., Auken, E., Fiandaca, G., 2018. Subsurface imaging of water electrical conductivity, hydraulic permeability and lithology at contaminated sites by induced polarization. Geophys. J. Int. 213, 770–785. https://doi.org/10.1093/gji/ggy018.

Maurya, P.K., Christiansen, A.V., Pedersen, J., Auken, E., 2020. High resolution 3D subsurface mapping using a towed transient electromagnetic system - tTEM: case studies. Near Surf. Geophys. 18, 249–259. https://doi.org/10.1002/nsg.12094.

Møller, I., Søndergaard, V.H., Jørgensen, F., Auken, E., Christiansen, A.V., 2009. Integrated management and utilization of hydrogeophysical data on a national scale. Near Surf. Geophys. 7, 647–659. https://doi.org/10.3997/1873-0604.2009031.

Pedersen, S.A.S., 2005. Structural analysis of the Rubjerg Knude glaciotectonic complex, Vendsyssel, northern Denmark. Geol. Surv. Denm. Greenl. Bull. 8, 192. https://doi.org/10.34194/geusb.v8.5253.

Rasmussen, E.S., Dybkjær, K., Piasecki, S., 2010. Lithostratigraphy of the upper Oligocene – Miocene session in Denmark. Geol. Surv. Denmark Greenl. Bull. 22, 93. https://doi.org/10.34194/geusb.v22.4733.

Rasmussen, P., Kallesøe, A.J., Sonnenborg, T.O., Sandersen, P., 2020. Geological and Hydrological Model for Sunds – Preventive Measures for Lowering the Groundwater Table now and in a Future Climate. A TOPSOIL Project Supported by the INTERREG

VB North Sea Programme. Geological Survey of Denmark and Greenland, p. 64. Report 2020/12.

Refsgaard, J.C., Auken, E., Bamberg, C.A., Christensen, B.S.B., Clausen, T., Dalgaard, E., Effersø, F., Ernstsen, V., Gertz, F., Hansen, A.L., He, X., Jacobsen, B.H., Jensen, K.H., Jørgensen, F., Jørgensen, L.F., Koch, J., Nilsson, B., Petersen, C., De Schepper, G., Schamper, C., Sørensen, K.I., Therrien, R., Thirup, C., Viezzoli, A., 2014. Nitrate reduction in geologically heterogeneous catchments - a framework for assessing the scale of predictive capability of hydrological models. Sci. Total Environ. 468–469, 1278–1288. https://doi.org/10.1016/j.scitotenv.2013.07.042.

Revil, A., Karaoulis, M., Johnson, T., Kemna, A., 2012. Review: some low-frequency electrical methods for subsurface characterization and monitoring in hydrogeology. Hydrogeol. J. 20, 617–658. https://doi.org/10.1007/s10040-011-0819-x.

Sandersen, P.B.E., Jørgensen, F., 2015. Neotectonic deformation of a late Weichselian outwash plain by deglaciation-induced fault reactivation of a deep-seated graben structure. Boreas 44, 413–431. https://doi.org/10.1111/bor.12103.

Sandersen, P.B.E., Jørgensen, F., 2017. Buried tunnel valleys in Denmark and their impact on the geological architecture of the subsurface. Geol. Surv. Denm. Greenl. Bull. 38, 13–16. https://doi.org/10.34194/geusb.v38.4388.

Sandersen, P.B.E., Jørgensen, F., Larsen, N.K., Westergaard, J.H., Auken, E., 2009. Rapid tunnel-valley formation beneath the receding late Weichselian ice sheet in Vendsyssel, Denmark. Boreas 38 (4), 834–851. https://doi.org/10.1111/j.1502-3885.2009.00105.x.

Sandersen, P.B.E., Jørgensen, F., Kallesøe, A.J., Møller, I., 2018. Opstilling af Geologiske Modeller til Grundvandsmodellering, Geo-Vejledning 2018/1 (Guidelines for Constructing Geological Models for Use in Groundwater Modelling). Geological Survey of Denmark and Greenland Special Publication (GEUS). ISBN 978-87-7871-497-8. www.geovejledning.dk.

Schamper, C., Jørgensen, F., Auken, E., Effersø, F., 2014. Assessment of near-surface mapping capabilities by airborne transient electromagnetic data: an extensive comparison to conventional borehole data. Geophysics 79 (4), B187–B199. https://doi.org/10.1190/geo2013-0256.1.

Sørensen, K., 1996. Pulled array continuous electrical profiling. First Break 14, 85–90.

Sørensen, K.I., Auken, E., 2004. SkyTEM – a new high-resolution helicopter transient electromagnetic system. Explor. Geophys. 35, 194–202. https://doi.org/10.1071/EG04194.

Thomsen, R., Søndergaard, V.H., Sørensen, K.I., 2004. Hydrogeological mapping as a basis for establishing site-specific groundwater protection zones in Denmark. Hydrogeol. J. 12, 550–562. https://doi.org/10.1007/s10040-004-0345-1.

Van der Vegt, P., Janszen, A., Moscariello, A., 2012. Tunnel Valleys: Current knowledge and future perspectives. In: Huuse, M., Redfern, J., Le Heron, D.P., Dixon, R.J., Moscariello, A., Craig, J. (Eds.), Glaciogenic Reservoirs and Hydrocarbon Systems, vol. 368. Geological Society of London Special Publication, pp. 75–97 (ISSN: 0305-8719).

Viezzoli, A., Auken, E., Munday, T., 2009. Spatially constrained inversion for quasi 3D modelling of airborne electromagnetic data an application for environmental assessment in the lower Murray Region of South Australia. Explor. Geophys. 40, 173–183. https://doi.org/10.1071/EG08027.

Viezzoli, A., Tosi, L., Teatini, P., Silvestri, S., 2010. Surface water-groundwater exchange in transitional coastal environments by airborne electromagnetics: the Venice Lagoon example. Geophys. Res. Lett. 37, L01402 https://doi.org/10.1029/2009GL041572.

Winsemann, J., Lang, J., Polom, U., Loewer, M., Igel, J., Pollok, L., Brandes, C., 2018. Ice-marginal forced regressive deltas in glacial lake basins: geomorphology, facies variability and large-scale depositional architecture. Boreas 47, 973–1002. https://doi.org/10.1111/bor.12317.